




Research on the Development of the Semi-Rigid Column Base of Reinforced Concrete: Experimental and Analytical Study on the Column Base with Cross Section Reduced Portion

Osamu Takahashi^{1*}, Hirona Yoshida², Minoru Od³

¹ Tokyo University of Science, 6-3-1, Nijuku, Katsushika-ku, Tokyo 125-8585, Japan 

² Tokyo University of Science, Nijuku, Katsushika-ku, Tokyo 125-8585, Japan 

³ Sumitomo Mitsui Construction Co., Ltd., Japan 

Received: / Accepted: 03.05.2020/05.06.2020

Abstract

Generally, in reinforced concrete buildings, joints have been planned as a rigid state due to the characteristics of their construction. In such a building, the stress of the first story column becomes nonuniform since the bending stress at the time of the earthquake is concentrated on the rigid joints of the foundation structure such as the column base at the first story. This paper proposed making the column base at the first story shape semi-rigid to reduce the stress concentrating on the column base at the first story. In order to realize semi-rigid column base, we performed structural experiments and FEM analysis on the column base with cross section reduced portion. As a result, it was concluded that the best structure shape is one with the cross section reduced portion and the taper at the column base as the semi-rigid column base with bending rigidity reduction and structural performance stability.

Key words: Reinforced concrete, column, semi-rigid, bending rigidity, burst stress

1. Introduction

1.1. Background

In order to design a structure rationally, it is desirable to have a frame that avoids localized collapse and concentration of deformation and resists well in balance over the building. The stress state of the structure subject to external force depends mainly on the rigidity of the member in the minute deformation region and the strength of the member in the large one. Since ordinary RC buildings adjust the cross-section area and the amount of reinforcement as members such as columns and beams against the existing stress, the rigidity and strength cannot be changed easily. If the rigidity and the strength of each member can be easily changed, it can be possible to design the building in a more rational stress state.

As a previous study carried out with such a purpose, there is the research ^[1] to make the connections of pile head semi-rigid. In the semi-rigid pile head method, the bending stress generated in the pile is equalized with respect to the entire pile by reducing the pile head rigidity,

* Corresponding Author,
e-mail: o.taka@rs.tus.ac.jp

realizing improvement in functionality and economical design. Here we develop the RC columns realizing a reasonable RC building by focusing on the 1st column of RC structure, controlling the bending stress state of it by reducing the column base rigidity.

1.2. Overview of Construction

Fig. 1 shows overview of this construction method. We compare the case of the ordinary column base, the case with semi-rigid spring and the case of actually designing it about the 1st column. In a high-rise building or the like, of the bending stress exists considerably on the column top. If a semi-rigid spring is provided on the column base without changing the shear force for design, the inflection point goes down and the bending stress of the column top and the column base approaches each other. However, from the viewpoint of seismic safety of the structure, it is necessary that as the actual semi-rigid detail, the strength of the column base does not decrease excessively.

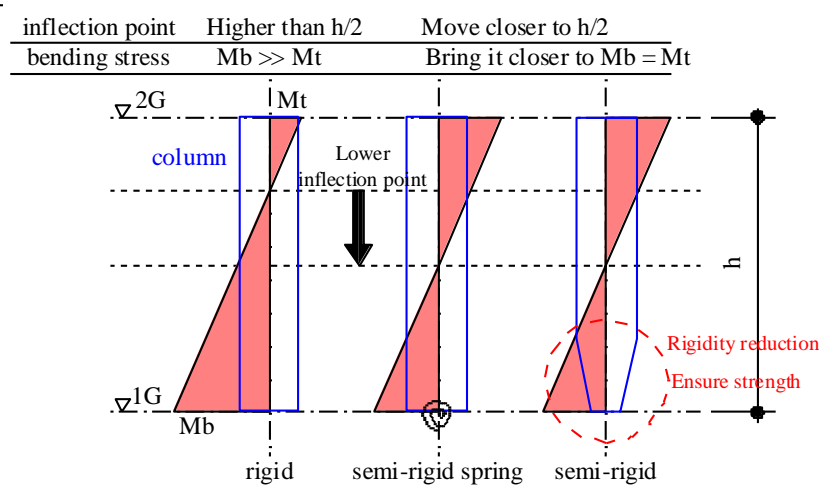


Figure 1. Overview of this construction

Fig. 2 shows an example of a stress diagram when the column base is rigid and semi-rigid. As in this example, when the height of the inflection point is fairly high, the bending stress of the column base is reduced by about 27% by the semi-rigid spring with the rigidity of 0.5. In actual design, stress reduction of 27% produces a significant difference on the reinforcement.

Fig. 3 shows the problems with previous columns. In the case where the inflection point is high and the column bending stress is large, there are roughly two ways to deal with it. From the figure, the case 1 is to change the cross section of the column against the existing stress on the first and second floors. In this case, a cross section switching part is required in the connection of column and beam on the second floor, so the reinforcement details become complicated. Thus, problems in construction tend to occur. The case 2 is to make the cross section of the column on the first floor and the second floor same. In this case, in order to cope with the existing stress, it is necessary to increase the amount of the reinforcing of the 1st column base, which makes it difficult to secure the main reinforcement interval and the like. For avoiding this problem, the cross-section area must be increased. In this construction method, the cross-section area of the column base is reduced and high strength concrete or the like is used, thereby reducing the rigidity of the column without excessively reducing strength.

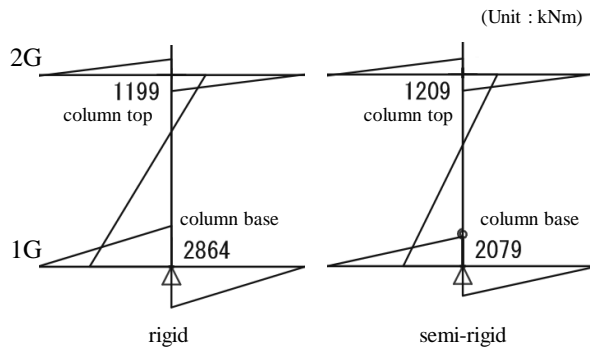


Figure 2. Example of bending stress diagram

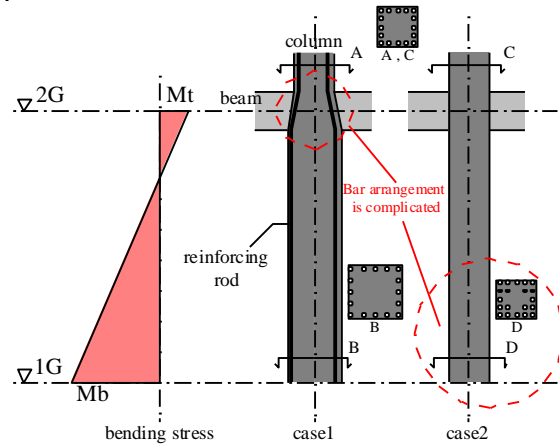


Figure 3. Problems of rigid columns

1.3. Effective scope

In order to understand the effective building with this construction method, elasticity analysis of the frame model was performed when the height and length of the building were changed, and the inflection point ratio of the representative intermediate column on the first floor was calculated.

Fig. 4 shows the relationship between the aspect ratio of each building and the inflection point ratio of the representative intermediate column on the first floor. Also, in the figure, the values of the actual design projects are plotted. The case where the inflection point ratio shows 0.5 is the case where the bending stress of the column top and the column base are equal, and all the analysis results are the inflection point ratio of 0.5 or more.

From the figure, there is a positive correlation between the aspect ratio and the inflection point ratio, and as the aspect ratio increases, the inflection point tends to rise. A similar tendency is seen also in the actual design example, and this construction method can be effectively applied to buildings with large aspect ratio and large influence of overall bending deformation. Especially, when the aspect ratio is 1.0 or more, the ratio of the inflection point ratio is about 0.75 or more, so the usefulness of this construction method is likely to be high.

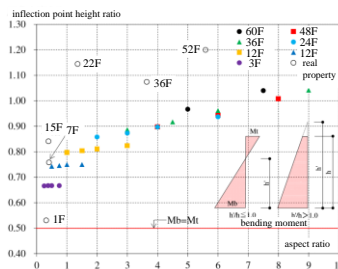


Figure 4. Relationship between aspect ratio and inflection point ratio

2. Experimental Study on RC Columns with Reduced Cross Section

In order to obtain the effect of reducing the rotational rigidity of the column base, a column specimen with a reduced part at the base was prepared and a bending shear experiment was conducted.

2.1. Specimen and method

Fig. 5 shows the specimen diagram and loading method, Table 1 the specimen list, and Table 2 shows the material test results. The specimen consists of a total of five bodies, a general column No. 1 having the same cross section in the axial direction, and columns No. 2 to 5 having a reduced part in the base. All the specimens were planned so that bending yield would precede.

In No. 2, there are two pairs of shear reinforcement (D6, SHD685), No. 3 and No. 5 steel pipes (STKR400, t=9mm) on the outer circumference of the reduced part, No. 4 steel plates (SS400, t=19mm) as two sheets. Here the high strength grout (Fc100) was filled in No. 2 itself, the steel pipe of No. 3 and 5, the lower surface of steel plate of No. 4 and the main reinforcement hole. In No. 5, the adhesion of the main reinforcement fixed in the column part was removed 300 mm by using a vinyl tube, thereby further reducing the rotational rigidity.

Table 3 shows the force cycle. The force was given a constant vertical force corresponding to the axial force ratio of 0.25 in the column part to the top, and positive and negative alternating loading was performed in the horizontal direction according to the loading cycle shown in the table.

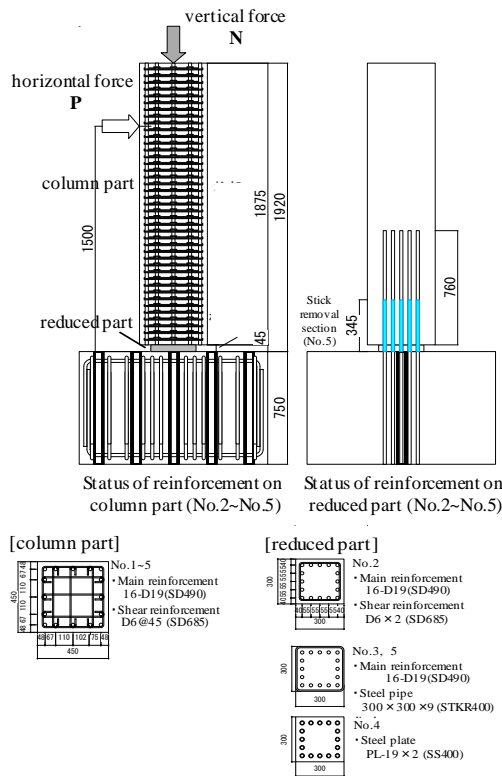


Table 1. List of specimens

specimen	cross section B x D (mm)	concrete strength Fc (N/mm ²)	column part reinforcement		axial force ratio η
			main p _d (%)	shear p _v (%)	
No.1					0.25
No.2	450	60	16-D19 (SD490)	5-D6@45 (SHD685)	N
No.3	450		p _d =2.16	p _v =0.79	B x D x σ_c x σ_B
No.4					
No.5					

specimen	cross section Br x Dr (mm)	concrete strength g Fc (N/mm ²)	reduced part reinforcement		constitution of cross section
			main p _d (%)	method	
No.1					
No.2	300	100	16-D19 (SD490)	2-D6 x 2 300 x 300 x 9	grout
No.3	300			PL-19 x 2	steel pipe
No.4	300			300 x 300 x 9	steel plate
No.5	300			STKR400	steel pipe + stick removal section

Table 2. Material test results

part	type material	yield point (N/mm ²)	yield strain (x 10 ⁻³)	elastic coefficient (x 10 ⁴ N/mm ²)
main reinforcement	D19 (SD490)	540	3182	1.93
	D6 (SHD685)	745	5957	1.90
shear reinforcement	PL9 (STKR400)	391	3750	2.06

type material	compressive stress (N/mm ²)	bursting stress (N/mm ²)	elastic coefficient (x 10 ⁴ N/mm ²)
concrete	57.7	3.05	3.53
grout	117.5	3.35	4.81

Table 3. Force cycle

R(rad)	Cycle
1/800	±2
1/400	±2
1/200	±2
1/100	±2
1/50	±2
1/25	±1

Figure 5. Specimen diagram and Loading method

2.2. Result and discussion

Fig. 6 shows the column base cracks of No. 1 and 3, Fig. 7 left shows the shear force - deformation angle relationship (considering the P-Δ effect) of No. 3 and the envelope of the shear force - deformation angle relationship of all specimens (considering the P-Δ effect), and Table 4 shows experimental result and calculated value of strength. Bending yield was preceded in all specimens and showed stable hysteretic properties until about 1/18 rad of large deformation. In the following, the experimental process of each specimen will be described.

In No. 1, bending cracks (①) at the column base at $1/400$ rad, shear cracks (②) $1/2 D$ (D : column part vertical width) away from the dangerous cross section position at $1/200$ rad, and lengthwise cracks (③) in the corner occurred. After that, rigidity declined, and the main reinforcement compression yielded at $1/50$ rad and the load became almost constant. In No. 3 using a steel pipe in the reduced part, lengthwise cracks (①) occurred at the center position of the lower in the column part at $1/200$ rad, the main reinforcement compression yielded at $1/100$ rad, then width cracking occurred, rigidity beginning to decline, and as the main reinforcement tension yielded at $1/50$ rad, the load became almost constant. Lengthwise cracks (①) occurred in all specimens with reduced part.

Fig. 7 right shows the initial rigidity (evaluation at $1/800$ rad from the origin) of each specimen. The rigidity reduction effect of the specimens No. 2 to 5 with the reduced part was about 54 to 69%. Among them, the rigidity reduction effect of No. 5 without the adhesion was 54%, which was larger than the other specimens.

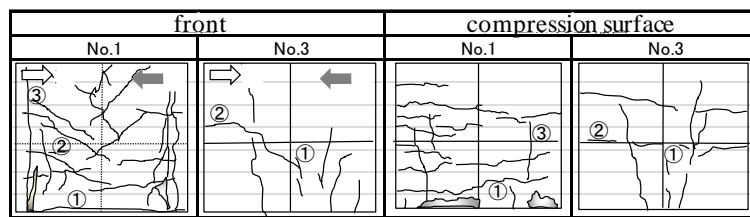


Figure 6. Crack of the column base

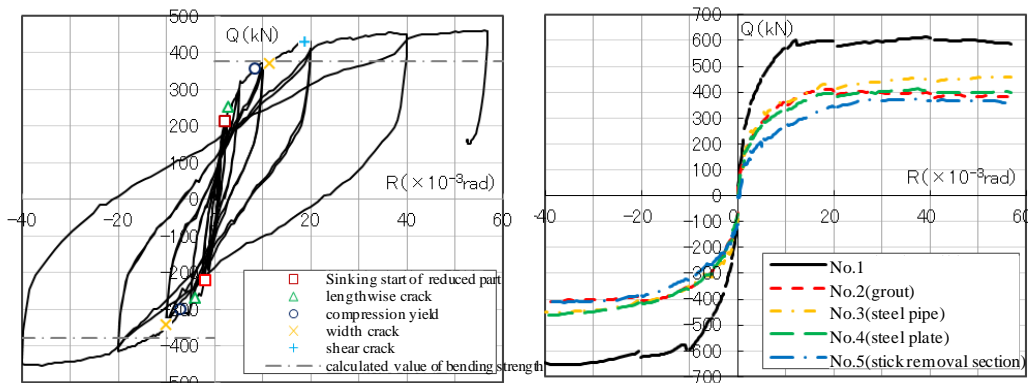


Figure 7. Shear force – deformation angle relationship (left: No.3, right: envelope)

Fig. 8 shows the transition of axial deformation. Axial deformation is the vertical displacement on the displacement meter placed at a height of 1500 mm from the base. In all specimens, axial deformation tended to increase due to the progress of the deformation angle and repetition with the same deformation after $1/100$ rad. Increase in axial deformation from the elastic state before given horizontal force to the end of $1/50$ rad was 0.54 mm (No. 1), 0.70 mm (No. 2), 1.04 mm (No. 3), 1.04 mm (No. 4), 0.87 mm (No. 5). From these values, in particularly No. 3 to 5 using a steel for the reduced part were larger than No. 1, which seemed to be contributed to the local crash at the contact between the steel and the concrete. In addition, lengthwise cracks generated in all specimens with reduced parts were due to tensile stress orthogonal to the local compressive stress, which confirmed this fact.

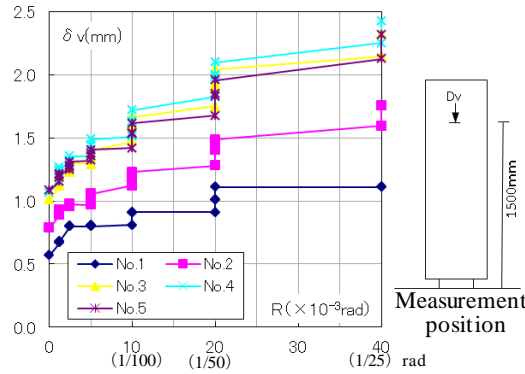


Figure 8. Transition of axial deformation

Table 4. Experimental result and calculated value of strength

specimen	crack										yield main reinforcement				maximum strength				calculated value			
	bending (+)		bending (-)		shear (+)		shear (-)		lengthwise (+)		lengthwise (-)		compressive (+)		compressive (-)		(+)	(-)	bending	she		
	Q (kN)	R (rad)	Q (kN)	R (rad)	Q (kN)	R (rad)	Q (kN)	R (rad)	Q (kN)	R (rad)	Q (kN)	R (rad)	Q (kN)	R (rad)	Q (kN)	R (rad)	Q (kN)	R (rad)	cQmu (kN)	cQsu		
No.1	272	1.5	-288	-1.7	453	5.0	-403	-3.8	567	9.4	-542	-8.7	581	12.5	-582	-12.0	614	39.4	-652	-35.4	576	91
No.2	170	1.5	-166	-1.3	—	—	-407	-20.0	350	8.7	-328	-7.7	359	10.0	-354	-10.0	411	19.0	-412	-38.7	377	
No.3	—	—	—	—	429	18.7	-451	-38.0	251	2.9	-270	-4.0	356	8.4	-300	-7.0	460	56.1	-453	-36.0	377	
No.4	—	—	—	—	376	14.7	-414	-18.4	173	1.7	-175	-1.7	319	8.3	-301	-7.3	413	37.4	-461	-38.0	377	
No.5	—	—	—	—	—	—	—	—	122	1.6	-182	-1.6	370	25.4	-397	-24.0	376	36.1	-412	-40.0	377	

※1 : R (× 10⁻³) ※2 : (+)Positive force , (-)Negative force ※3 : lengthwise cracks of No. 1 are co

3. Analytical Study on Internal Stress

We describe the result of FEM analysis for the purpose of clarifying the cause of lengthwise cracks which was the subject of the experiment. Among the specimens mentioned in Chapter 2, one of the subject was the general column (No. 1) and the other had a reduced part in the column base (No. 2). In addition, we proposed a new structural shape to prevent lengthwise cracks and investigate effective reducing cross section method by analyzing it. For the analysis, MIDAS/iGen, structural analysis software, was used to perform static incremental loading applying horizontal force while exerting a constant vertical force.

3.1. Analysis model and method

Fig. 9 shows the outline of the analysis model, and Fig. 10 shows the list of analysis model including the new structural shape. We performed material nonlinear analysis by modeling concrete with solid elements and reinforcing rods with truss elements. The adhesion of concrete and reinforcing rods was assumed to be adequate, and reinforcing rods was not taken out. The breakdown criterion of Mohr-Coulomb was used for the yield survey of concrete, and the yield condition of Von Mises was used for that of reinforcing rods, and the rigidity of the reinforcing rods after the yield was 1/100 of the elastic rigidity.

As an analysis model, we prepared an experimental model that reproduced the specimens (No. 1, No. 2) to reproduce experiments of Chapter 4 and a real model to examine new structure shapes. For the real model, we used the composition rule that gained validity in the experimental model. As a new structural shape, we proposed the followings, No. 3 to reduce the bending stress of the lengthwise cracks generation position by raising the cross section switching part, No. 4 to eliminate abrupt cross-sectional change by providing the tapered part at the cross section switching part, and No. 5 to provide the tapered part on the foundation.

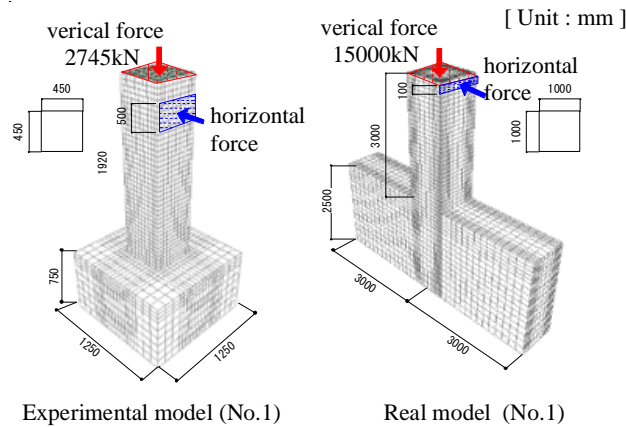


Figure 9. Analysis model

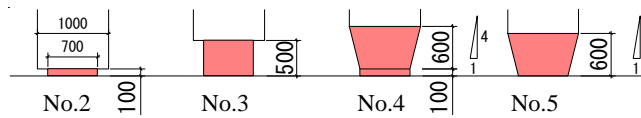


Figure 10. analysis models

3.2. Result and discussion

Fig.11 shows the comparison of shear force – deformation angle relationship between the experimental model and experimental results. In both No. 1 and No. 2, the experiment result and the analysis result are in good agreement, and the validity of the analysis model can be confirmed.

The lengthwise cracks occur at a position where tensile principal stress generating larger than the burst strength (tensile strength) in a direction orthogonal to the principal stress direction. As shown in Fig. 12, the lengthwise cracks of No. 2 occurred earlier in the analysis result. This is considered to have occurred earlier than the actual recording because it was determined visually in the experiment. In addition, it can be said that the reproducibility is high because the analysis result was in good agreement with the lengthwise cracks at the time of experiment such as occurrence place, direction.

Next, we compared and examined by the structure shape. Fig. 13 shows the comparison of shear force – deformation angle relationship by the structure shape. The effect of the reducing rigidity can be confirmed in all the semi-rigid models (No. 2 to 5) against No. 1. For No. 2 and No. 3 with the abrupt cross-sectional change, the occurrence of lengthwise cracks was delayed in No. 4 and 5 with a tapered part. In addition, lengthwise cracks were generated almost in the elastic range.

Therefore, in the next chapter, the difference in the occurrence of lengthwise cracks due to the structural shape will be quantitatively understood from the results of elastic analysis.

3.3. Estimation of maximum bursting stress and comparison by shape

Fig. 14 shows the comparison of the maximum principal stress distribution. The burst stress that causes lengthwise cracks was distributed at the maximum immediately above the end of the reduced part on the compression side, which was common to all of No. 2 to 5. Also, in No. 4 and 5, the maximum burst stress was small and the occurrence of lengthwise cracks considered to be delayed, which was consistent with the result in the previous chapter. For this maximum burst stress ($\sigma_{y_{max}}$), elasticity analysis of 120 patterns was performed based on the

analysis parameters shown in Fig. 15 to obtain an estimation equation (1)

$$\sigma_{ymax} = k_1 t_1 \frac{N}{A} + k_2 t_2 \frac{M}{Z} \quad (1)$$

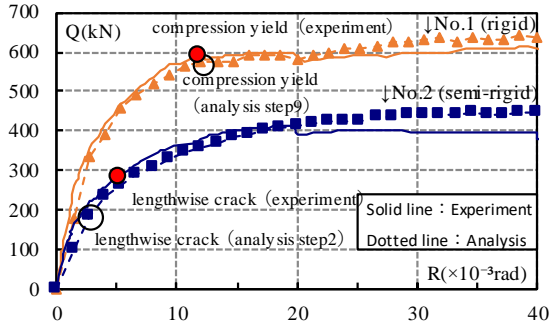


Figure 11. Comparison of shear force – deformation angle relationship

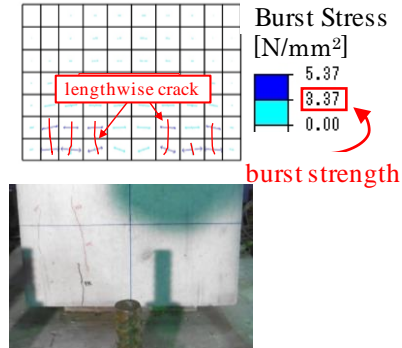


Figure 12. Comparison of length wise crack

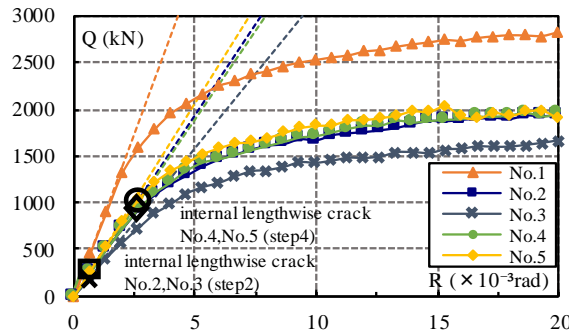


Figure 13. Comparison of shear force – deformation angle relationship by structure shape

Here, k_1 and k_2 are shape factor determined by the reduction ratio and the aspect ratio of the reduced part, and t_1 and t_2 are taper factor determined by the taper angle when taper is given (without taper, $t_1=t_2=1.0$). Each of them can be obtained by their structure shape using Fig. 16 and 17.

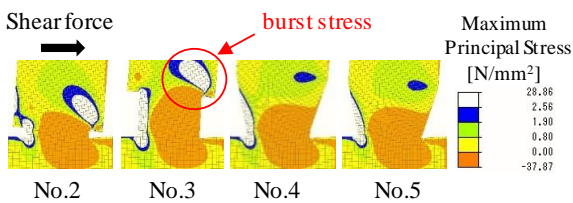


Figure 14. Comparison of maximum principal

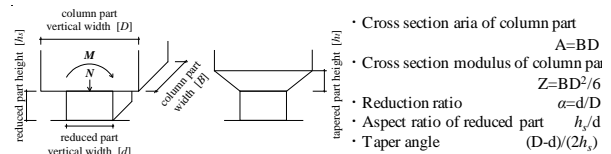


Figure 15. Analysis parameters

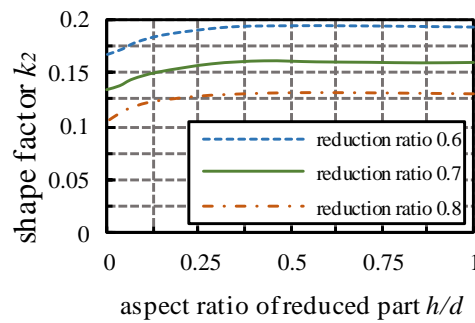
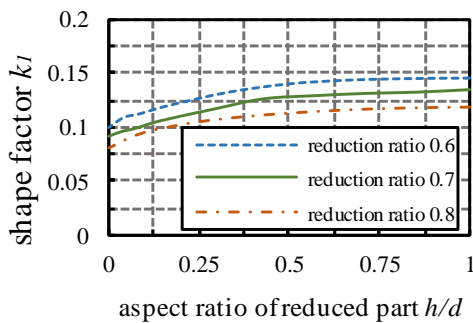


Figure 16. Relation between shape factor k and shape

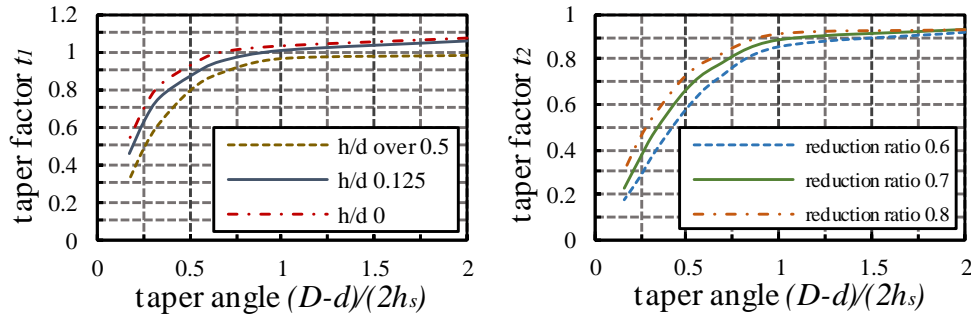


Figure 17. Relation between taper factor t and shape

The lengthwise cracks due to the difference in the structural shape was investigated by the equation (1). The axial force ratio was 0.25 with respect to the column part, and the lengthwise cracks criteria was 1.5 times the bending cracking moment. Now we compared the maximum burst stress for each structural shape determined by axial force and switching part moment at that time.

Fig. 18 shows the results of determination of occurrence of lengthwise cracks. It said that the effect of decreasing the maximum burst stress was small when the switching part was raised. Also, the difference due to the reduction ratio was small. On the other hand, it was found that the reduction effect was large when the tapered part was added and the taper angle was decreased. Especially, when the taper angle was $4/12$ or less, the maximum burst stress was smaller than the burst strength, so lengthwise cracks could be suppressed.

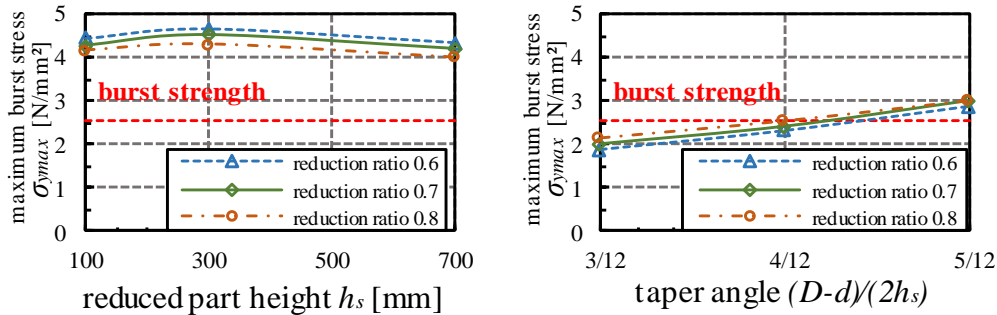


Figure 18. Determination of occurrence of lengthwise cracks

4. Experimental Study on RC Columns with Tapered Part

In the FEM analysis of the previous chapter, it was found that lengthwise cracks can be mitigated by providing a tapered part between the column part and the reduced part. Therefore, we conducted experiment aimed at grasping the control effect of lengthwise cracks and the rigidity reduction effect in the case where the tapered part is provided and the case where the reduced part is extended in the height direction.

4.1. Specimen and method

Table 5 shows the list of specimens. The specimen consists of a total of three bodies, the two with the tapered part whose taper angle are changed and the one with the extended reduced part. Fig. 19 shows specimen diagram. The upper part of Fig. 19 shows the column part, and the lower part shows the tapered part and the reduced part.

As shown in Table 5 and Fig. 19, the reduction ratio in each specimen is 0.8. The taper angle of two specimens is 4/12 (No. 6) and 6/12 (No. 7). Each height of the reduced part is 45 mm.

Table 6 shows the material test results. The concrete strength is Fc60 in the column part and Fc100 in the reduced part and tapered part. The experiment method is the same with chapter 2.

4.2. Result and discussion

Table 7 shows the list of experimental results, Fig. 20 shows the occurrence of initial cracks, Fig. 21 shows the shear force – deformation angle relationship and the cracking situation at 1/50 rad.

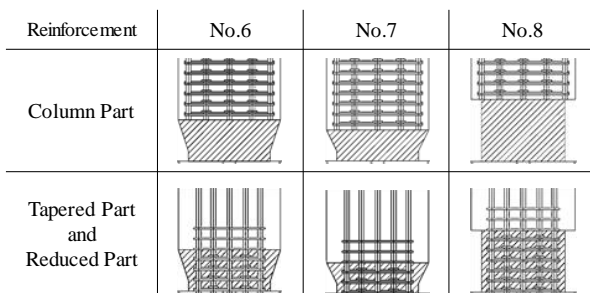
In No. 6, firstly, bending cracks (①) occurred in the reduced part, secondly, lengthwise cracks (②) occurred in the corner of compression surface, and finally, lengthwise cracks (③) occurred in the column part and the tapered part at 1/186 rad, which is considerably larger than 1/400 of the previous specimens without taper. The initial rigidity was 10.72×10^4 kN/rad.

In No. 7 and 8, the order between cracks (②) and (③) was invers against No. 6. The deformation angle when lengthwise cracks occurred in the column part was 1/306 (No. 7) and 1/538 (No. 8). The initial rigidity was 10.90×10^4 kN/rad (No. 7) and 9.58×10^4 kN/rad (No. 8).

Table 5. List of specimens

specimen	column part						other		
	cross section			concrete strength Fc (N/mm ²)	reinforcement				
	B (mm)	D (mm)	Lg (mm)		main p _t (%)	shear p _w (%)			
No.6	450	450	1740	60	16-D19 (SD490)	5-D6@45 (SHD685)	Same as previous experiment		
No.7			1785					p _t =0.79	p _w =0.78
No.8			1650						
specimen	reduced part						constitution of cross section		
	cross section			concrete strength g Fc (N/mm ²)	reinforcement				
	Br (mm)	Dr (mm)	Ls (mm)		main p _t (%)	shear p _w (%)			
No.6	360	360	180	100	16-D19 (SD490)	4-D6@45 (SHD685)	Reduction ratio 0.8 , Taper angle 4/12		
No.7			135				Reduction ratio 0.8 , Taper angle 6/12		
No.8			270				Reduction ratio 0.8		

Lg : The length from the part change point to the top of the specimen , Ls : The length from the column base to the part change point
 ※Set a height of 45 mm in the column base of No. 6 and No.7



※Shaded part is Fc100

Figure 19. Specimens diagram

Table 6. Material test result

part	type material	yield point (N/mm ²)	yield strain ($\times 10^{-6}$)	elastic coefficient ($\times 10^5$ N/mm ²)
main reinforcement	D19 (SD490)	533	2916	1.94
shear reinforcement	D6 (SHD685)	724	3888	1.86
part	compressive stress (N/mm ²)	bursting stress (N/mm ²)	elastic coefficient ($\times 10^4$ N/mm ²)	
column	69.0	4.05	3.31	
taperd and reduced	92.8	4.81	3.79	

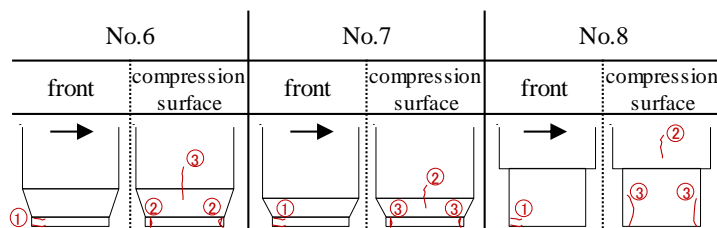


Figure 20. Initial crack progress diagram

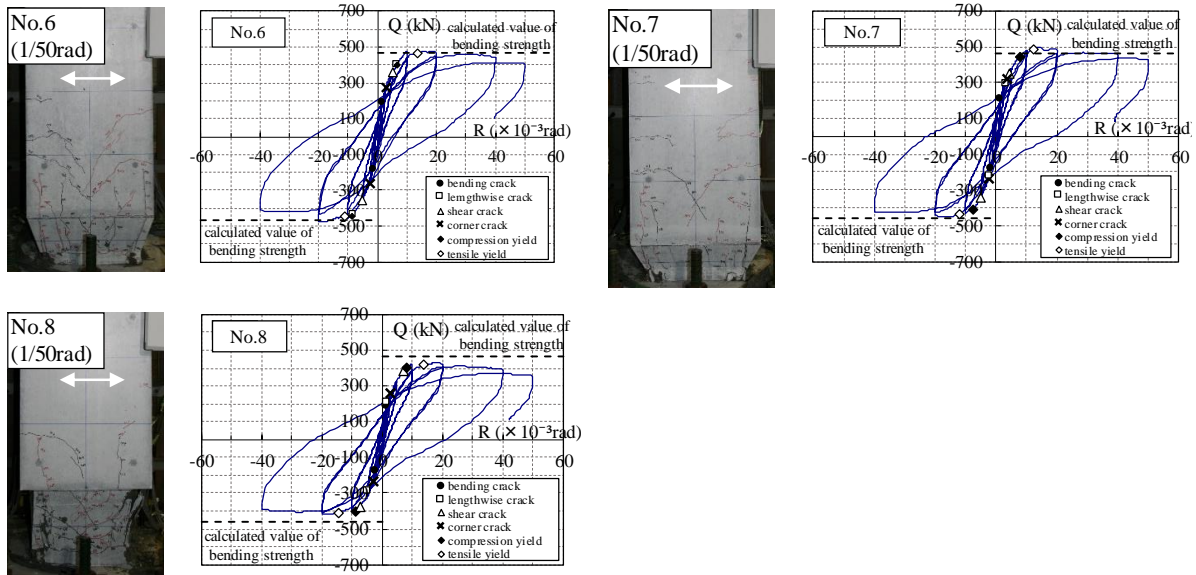


Figure 21. Shear force – Deformation angle relationship

Fig. 22 shows the comparison of envelopes. In the figure, a general column (No. 1) of previous specimen is superimposed as a reference value. From the figure, the rigidity and strength of each specimen are lower than No. 1. By providing the reduced part and the tapered part, the rigidity of the column base was reduced.

Fig. 23 shows the transition of axial deformation. The axial deformation of each specimen was nearly equivalent. This value is about twice as large as that of No.1 without the reduced part. This axial deformation is an influence due to the reduction of the cross-section area, and the situation where the reduced part is pushed into the column part was not confirmed.

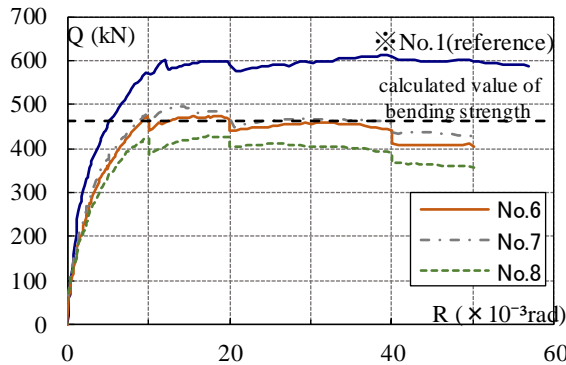


Figure 22. Comparison of envelopes

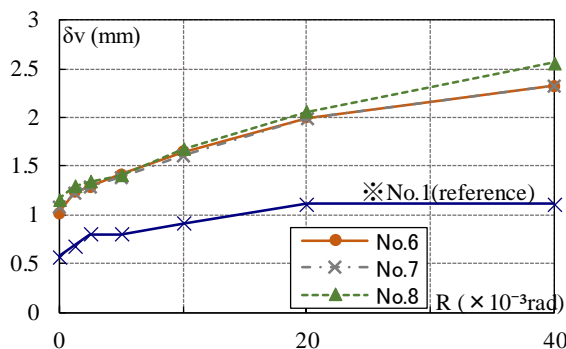


Figure 23. Transition of axial deformation

Conclusions

In this paper, the problems of the general design method are shown, and the semi-rigid base RC column is proposed as the solution. In addition, the following findings were obtained from experiments and analysis on the semi-rigid column base

- 1) By providing a reduced part on the column base, the initial rigidity can be reduced to 60~70% with respect to the general column.
- 2) When a steel is used for the reduced part, local crash occurs and axial deformation progresses.
- 3) When the reduced part is provided, burst stress occurs at the cross section switching part and lengthwise cracks occur. As a method to solve this problem, it is effective to provide a tapered part having a taper angle of 4/12 or more.

From the above findings, it is concluded that by providing the tapered part and the reduced part in the column base, it has stable structural properties and it is possible to reduce the rigidity.

Acknowledgements

I wish to acknowledge Sumitomo Mitsui Construction Co., Ltd. for their assistance in conducting this research. Also, I wish to thank Takei Sotaro for doing this research together and for teaching us many things.

References

- [1] Yoshimatsu Toshiyuki, Nishimura Noriyoshi, Konomi Mitsuo, Isemoto Noriaki, Yamaura Ichiro, Uozumi Masashi et al. "Development of Semi-rigid Connections for Cast-in-place Pile Head." Summaries of technical papers of annual meeting Architectural Institute of Japan. 2006; Structural 4: 349-366.
- [2] Nagashima Ryutaro, Oda Minoru, Hirata Yuichi, Tano Kenji, Ito Akira and Takaoka Yuji. "An Analytic Study on Semi-rigid Connections for Pile top, Foundation Beam and Column Bottom of First Floor." Summaries of technical papers of annual meeting Architectural Institute of Japan. 2015; Structural 4: 589-590.
- [3] Hirade Tsutomu, Sugimura Yoshihiro, Funayama Hikoshiro, Satio Tadashi and Murakami Masakatsu. "Experimental Study on Pile Head Joint of High Rotational Freedom System." Summaries of technical papers of annual meeting Architectural Institute of Japan. 1999; Structural 4: 527-528